ELSEVIER

Polymer 40 (1998) 27–33

polymer

# Solid-state n.m.r. investigation of crosslinkable blends of novolac and poly(ϵ-caprolactone)

Zhikai Zhong, Qipeng Guo[1], Yongli Mi*

*Department of Chemical Engineering, The Hong Kong University of Science and Technology, Clear Water Bay, Kowloon , Hong Kong*

Received 7 November 1997; revised 23 February 1998; accepted 17 March 1998

**Abstract**

The miscibility, phase behavior, and intermolecular interaction of novolac/poly(ϵ-caprolactone) (PCL) blends, before and after curing, were investigated by the high resolution solid-state nuclear magnetic resonance (n.m.r.) technique. It was found that there exists hydrogen-bonding interaction between the carbonyl groups of PCL and the hydroxyl groups of novolac, which results in the downfield shift of carbonyl carbon resonance of PCL and the upfield shift of hydroxyl-substituted carbon resonance of novolac. The interaction also broadens the line width of carbonyl carbon resonance. After curing with 15 wt% hexamine (relative to novolac content), hydrogen-bonding interaction still exists between the components in the crosslinked blends. However, the relative amount of hydrogen bonds decreases significantly. Both the uncured and the cured novolac/PCL blends exhibit composition-dependent miscibility. The curing causes an increase of the domain size in the amorphous phase and a reaction of miscibility between the two components. 

*Keywords:* Novolac resin; Poly(ϵ-caprolactone); Polymer blends

## 1. Introduction

For several decades, polymer blends have been studied quite extensively, and for certain systems, intensive studies have also been carried out. Considerable applications were witnessed in the 80s and 90s. In the process of utilization and development of polymer blends, a variety of techniques were used to study and characterize miscibility and phase behavior of polymer blends [1–4], among which, thermal analysis is the most widely used technique by researchers. Spectroscopic methods have also received more and more attention in recent years. One of the spectroscopic techniques that is frequently used in studying polymer blends is solid-state nuclear magnetic resonance (n.m.r.) [5–18]. By examining n.m.r. spectra and parameters, such as the chemical shift, line width, and relaxation times, one can obtain detailed information about the miscibility, intermolecular interaction, and morphology of polymer blends. Changes in chemical shift and/or line shape of the resonance peaks in the $^{13}C$ n.m.r. spectra of the blends, in comparison to those of the pure components, were employed as evidence of interaction between the blend components [8–12,18]. From n.m.r. relaxation time measurements, one can further estimate the scale of miscibility of a polymer blend.

Polymer blends of novolac and poly(ϵ-caprolactone) (PCL) have previously been studied by using differential scanning calorimetry (DSC) and Fourier transform infrared (FTIR) spectroscopy [19]. We have found that the uncured novolac/PCL blends were miscible as shown by the existence of a single glass transition temperature ($T_g$) in each blend. After being cured with 15 wt% hexamine (relative to novolac content), no $T_g$ can be detected for novolac-rich compositions. The miscibility was judged from the melting and crystalline behavior of the blends, and composition-dependent miscibility was found. Our *FTi*.r. studies revealed that there exists hydrogen bonding interaction between the hydroxyl groups of novolac and the carbonyl groups of PCL in the uncured novolac/PCL blends, and the curing reduced the intermolecular hydrogen-bonding significantly.

In this work, both the uncured and the cured novolac/PCL blends were further investigated by solid-state n.m.r. spectroscopy. The cross-polarization (CP) and magic angle spinning (MAS) technique together with the high-power dipolar decoupling (DD) technique was used to

* Corresponding author.

[1] Present address: Department of Polymer Science and Engineering, University of Science and Technology of China, Hefei 230026, Anhui, P. R. China

0032-3861/98/$ - see front matter 
PII: S0032-3861(98)00242-0

obtain high resolution $^{13}C$ spectra and to study the intermolecular interaction. In addition, the proton spin-lattice relaxation times were measured to determine the miscibility scale of the blends and the effect of curing on the miscibility of the blends.

## 2. Experimental

### 2.1. Materials and preparation of samples

The poly(ϵ-caprolactone) (PCL, Placcel H-7) was purchased from Daicel Chemical Ind., Ltd, Japan; it had a number-average molecular weight, Mn, of 70 000–100 000. The novolac was obtained from Hefei Perfumery Factory, Hefei, China; it had a number-average molecular weight, Mn, of 565 determined by vapor phase osmometry. The novolac was used without further purification. Hexamine (hexamethylenetetramine, HMTA) was chemically pure and was used as crosslinking agent.

All the blend samples were prepared by solution casting using methylene chloride/ethanol (90/10 by volume) as common solvent for both polymers. The solvent was almost completely evaporated at ambient temperature, then the samples were dried at 50°C in a vacuum oven for 72 hr to remove the residual solvent. Novolac/PCL blends were cured with 15 wt% HMTA relative to the content of novolac in the blends, i.e., with HMTA/novolac = 0.15. The curing was performed successively at 100°C for 2 hr, at 150°C for 2 hr, and finally at 190°C for 2 hr.

### 2.2. High-resolution solid-state n.m.r.

The $^{13}C$ n.m.r. experiments were carried out at ambient temperature (27°C) with a JEOL EX-400 spectrometer operating at resonance frequencies of 399.65 MHz for $^{1}H$ and 100.40 MHz for $^{13}C$. The high-resolution solid-state $^{13}C$ n.m.r. spectra were obtained by using CP/MAS/DD technique. The total sideband suppression (TOSS) pulse sequences were employed to suppress the spinning side bands when measuring $^{13}C$ n.m.r. spectra. The 90° pulse with width of 5.5 μs was employed with free induction decay (FID) signal accumulation, and the CP Hartmann–Hahn contact time was set as 1000 μs for all experiments because this contact time was experimentally demonstrated as suitable for the detection of CP/MAS/DD n.m.r. spectra for both novolac, PCL and their blends. The Hartmann–Hahn CP matching and dipolar decoupling field strength was 40 kHz, and the rate of MAS was 5.5 kHz for measuring both $^{13}C$ spectra and relaxation time. The recycle delay time was chosen in the range 5–10 s, depending on the relaxation behavior of the sample investigated. The $^{13}C$ chemical shifts were calibrated by taking the $^{13}C$ chemical shift of the methine carbon of solid adamantine (29.5 ppm relative to TMS) as an external reference standard.

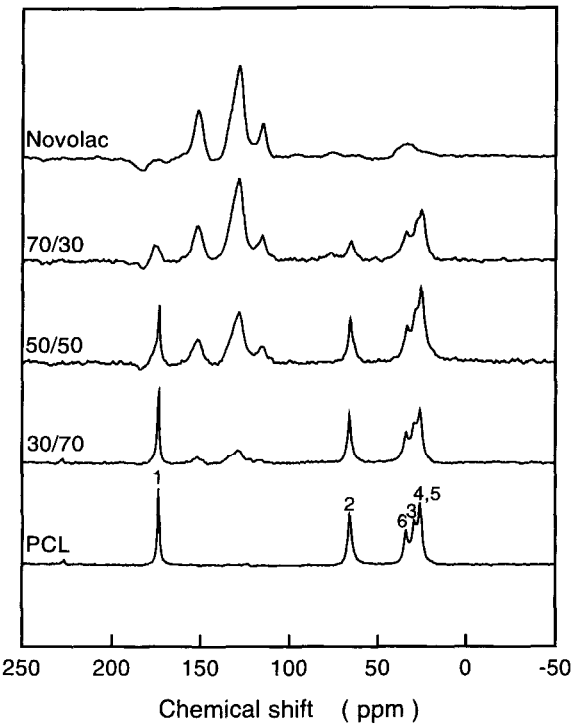


Fig. 1. $^{13}C$ CP/MAS/DD spectra of the uncured novolac/PCL blends.

The proton spin-lattice relaxation times in the laboratory frame, $T_1(H)$, were measured by monitoring the decay of specific carbon resonance intensities after $\pi-\tau-\pi/2$ pulse sequence using the inversion-recovery (i.r.) method. The proton spin-lattice relaxation times in the rotating frame, $T_{1\rho}(H)$, were determined by observing the carbon signal intensities with a $^{1}H$ matched spin-lock pulse sequence prior to cross polarization (spin-locking method).

## 3. Results and discussion

### 3.1. Uncured novolac/PCL blends

The $^{13}C$ CP/MAS/DD spectra of uncured novolac, PCL and their blends are shown in Fig. 1. Four peaks were observed for the uncured novolac. The resonance line at 153 ppm is caused by the hydroxyl-substituted carbon in phenol ring (C–OH). The peaks at 116 ppm and 129 ppm are correspondent to the ortho-unsubstituted carbons and the other carbons in the phenol ring, respectively. The other resonance line at 33 ppm corresponds to the methylene carbons. The $^{13}C$ n.m.r. spectra of PCL have five resonance lines and are assigned as the following:

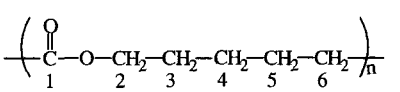

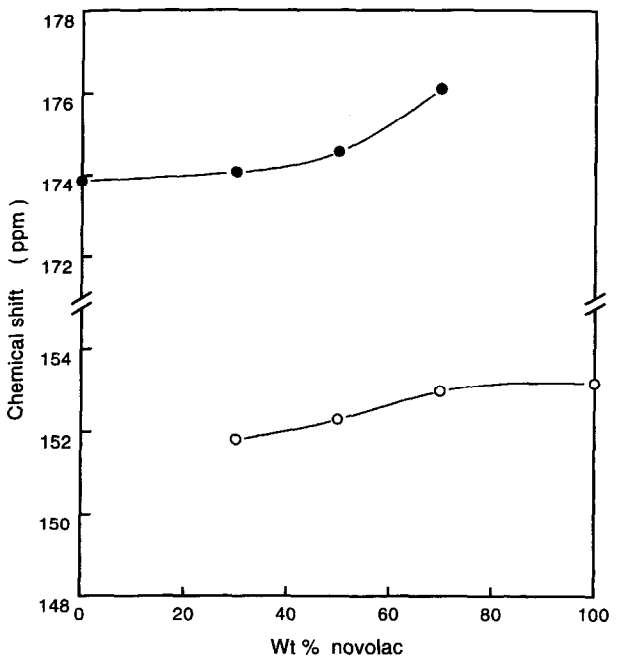


Fig. 2. Composition dependence of chemical shifts of the carbonyl carbon and the hydroxyl-substituted carbon resonances in the uncured novolac/PCL blends.

It should be pointed out that the PCL spectra are better than those of novolac. One of the reasons is that novolac is a industrial product whereas PCL has higher purity. Additionally, for the purpose of comparing, the experimental conditions for both pure components and their blends were the same; the conditions may be more suitable for PCL. Therefore, the spectra of PCL have a relatively higher intensity and hence better signal-to-noise than those of novolac.

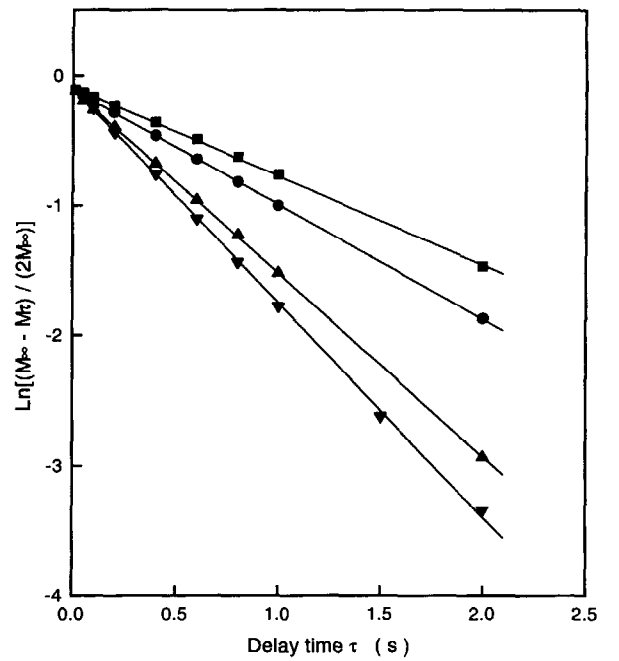


Fig. 3. Plots of $\ln[(M_\infty - M_\tau)/(2M_\infty)]$ against delay time (at selected chemical shift (26 ppm) for the uncured novolac/PCL blends. Novolac/PCL: 0/100 (■), 30/70 (◎), 50/50 (▲), and 70/30 (▼).

For the spectra of the uncured novolac/PCL blends, it is noted that there are some overlaps of resonances at about 33 ppm because both novolac and PCL have resonance signals in this chemical shift range. The intensities of the resonance peaks change regularly with the variation of composition, and the peaks of novolac become rather weak for the 30/70 novolac/PCL composition. It can further been found that the chemical shifts of the carbonyl carbon (C=O) of PCL and the hydroxyl-substituted carbon of novolac also change monotonically with composition. The variation in chemical shift may indicate the intermolecular specific interaction between the components [8–12,18]. This phenomenon was therefore carefully studied and the results are plotted in Fig. 2. As shown in Fig. 2, the carbonyl carbon resonance of PCL component shifts downfield as novolac increases in the blends, and this indicates the existence of intermolecular hydrogen-bonding interaction. It is well known that bond angle and intrachain distance of nearest neighbour are expected to change after the formation of specific interaction [20]. Therefore, the correlative carbon would experience a different chemical environment, which would change the magnetic shielding and hence the chemical shift. The shift of the carbonyl carbon in the 70/30 novolac/PCL blend is 2.2 ppm relative to that of the pure PCL, which is comparable to that of other hydrogen-bonded miscible blends [9–12]. It can also be found from Fig. 1 that the line width of the C=O carbon broadens significantly with the increase of novolac content in the blends and this is caused by a distribution of both bonded and nonbonded C=O carbon resonances. Similar shift of resonance line was also found for the hydroxyl-substituted carbon of novolac. However, the C–OH resonance line shifts upfield, not downfield, as PCL increases its concentration in the blends. This is probably because the formation of hydrogen bonds between the carbonyl groups of PCL and the hydroxyl groups of novolac influences the electron density around the carbons bearing the specific interaction, and gives rise to the variation of weak magnetic shield to the hydrogen-bonded carbonyl carbon whilst a strong magnetic shield to the hydroxyl-substituted carbon remains. Therefore, the chemical shift changes in different directions for the C=O carbon and the C–OH carbon. The results presented here are consistent with our previous study on these blends using *FT*i.r. technique [19]. The spectral changes caused by the blending also suggest an intimate mixing of polymer chains of the two components.

Neighbouring protons in polymer chains usually relax at an identical rate because of dipolar coupling. In contrast, protons far apart or in different environments relax independently of one another. It is thus possible, from the relaxation rates of protons belonging to two different polymers, to determine the homogeneity of mixing in a polymer blend. In the $T_1(H)$ experiment, the inversion recovery method was

Table 1
$T_1(H)$ values for uncured novolac, PCL, and their blends[a] (unit: s)

| | PCL | Novolac | | | PCL | PCL/ novolac | PCL | |
|---|---|---|---|---|---|---|---|---|
| PCL/ novolac | 174 ppm | 152 ppm | 129 ppm | 116 ppm | 66 ppm | 34 ppm | 29 ppm | 26 ppm |
| 100/0 | 1.50 | | | | 1.45 | 1.43 | 1.42 | 1.46 |
| 70/30 | 1.04 | 1.16 | 1.09 | – | 1.01 | 1.22 | — | 1.19 |
| 50/50 | 0.83 | 0.87 | 0.80 | – | 0.73 | 0.77 | — | 0.71 |
| 30/70 | 0.68 | 0.69 | 0.66 | 0.67 | 0.61 | 0.65 | — | 0.61 |
| 0/100 | | 0.59 | 0.53 | 0.52 | | 0.53 | | |

[a]The accuracy of the measurements is ± 5%

used, and the resonance intensities of novolac, PCL, and their blends were measured as functions of delay time. According to the method used, the magnetization of resonance relaxed at single exponential function should obey the following exponential equation:

$$M_\tau = M_\infty[1 - 2\exp(-\tau/T_1(H))] \quad (1)$$

where $T_1(H)$ is the proton spin-lattice relaxation time in the laboratory frame; $\tau$ is the delay time used in the experiment and $M_\tau$ is the corresponding resonance intensity; $M_\infty$ is the intensity of the resonance at $\tau \geq 5T_1(H)$. Taking the natural logarithm of both sides of Eq. (1), Eq. (2) can thus be obtained:

$$\ln[(M_\infty - M_\tau)/(2M_\infty)] = -\tau/T_1(H) \quad (2)$$

Plotting $\ln[(M_\infty - M_\tau)/(2M_\infty)]$ against $\tau$ will yield $T_1(H)$.

The plots of $\ln[(M_\infty - M_\tau)/(2M_\infty)]$ versus $\tau$ for the selected carbon (at 26 ppm) of PCL and novolac/PCL blends are shown in Fig. 3. It can be found that the experimental data fit Eq. (2) quite well at the whole selected delay time range and only one straight line was obtained for each composition. From the slope, $T_1$(H) was calculated. The values of $T_1(H)$ for the resonances of all carbons in novolac, PCL and their blends are summarized in Table 1. As expected, a single and composition-dependent of $T_1(H)$ was found for the uncured novolac/PCL blends, which is between those of the two pure components. In addition, the $T_1(H)$ values of all carbon resonances for each blend remain the same as far as experimental error is concerned. These results indicate that a fast spin-diffusion occurs among all protons in these blends, which averages out the whole

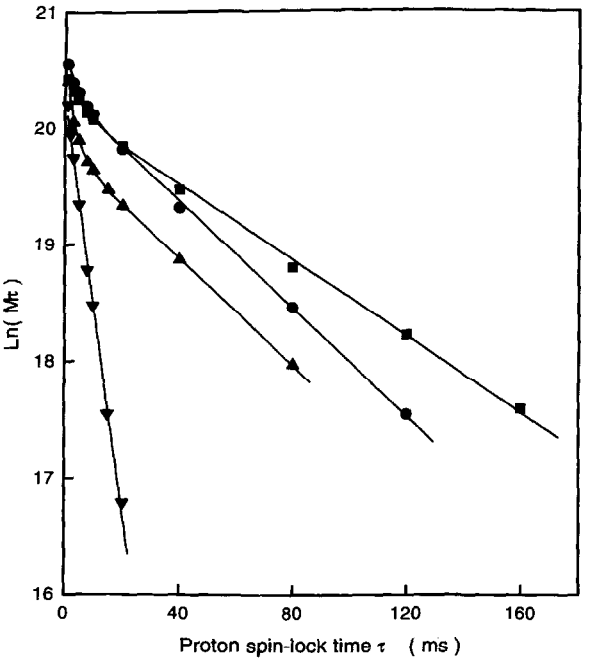


Fig. 4. Proton $T_{1\rho}$(H) relaxation behavior at the selected chemical shift (26 ppm) for the uncured novolac/PCL blends. Novolac/PCL: 0/100 (■), 30/70 (●), 50/50 (▲), and 70/30 (▼).

relaxation process. Thus, the domain size of these blends is smaller than the spin-diffusion path length within $T_1(H)$ time. For complete averaging over the time of relaxation, the upper limit of the spin-diffusion path length can be estimated using the following equation [21–23]:

$$L = (6DT_i(H))^{1/2} \quad (3)$$

where $D$ is the effective spin-diffusion coefficient depending on the average proton to proton distance as well as dipolar interaction and it has a typical value of the order of $10^{-16}$ m$^2$ s$^{-1}$. $T_i(H)$ is relaxation time ($T_1(H)$ or $T_{1\rho}(H)$, whereas for $T_{1\rho}(H)$, $D$ is scaled by a factor of 1/2 according to the relaxation experiment. On the basis of $T_1(H)$, it is believed that the uncured novolac and PCL are intimately mixed on a scale less than 20–30 nm.

As to the $T_{1\rho}(H)$ experiment, some interesting results were found. Based on the spin-locking mode employed in this measurement, the magnetization of resonance is expected to decay according to the following exponential

Table 2
$T_{1\rho}(H)$ values for uncured novolac, PCL, and their blends[a] (unit: ms)

| | PCL | Novolac | | | PCL | PCL/novolac | PCL | |
|---|---|---|---|---|---|---|---|---|
| PCL/novolac | 174 ppm | 152 ppm | 129 ppm | 116 ppm | 66 ppm | 34 ppm | 29 ppm | 26 ppm |
| 100/0 | 40.5/65.6 | | | | 34.5/63.3 | 28.8/62.1 | 26.8/62.6 | 24.6/64.5 |
| 70/30 | 23.4/45.8 | — | 1.55 | — | 19.8/43.9 | 16.2/40.1 | 15.7/41.0 | 16.2/44.3 |
| 50/50 | 13.5/58.5 | 2.44 | 2.28 | — | 11.1/54.6 | 7.20/60.0 | 7.36/54.2 | 7.80/48.0 |
| 30/70 | 6.50 | 6.45 | 6.30 | 6.33 | 6.02 | 6.23 | — | 5.59 |
| 0/100 | | 6.50 | 6.64 | 6.59 | | 6.62 | | |

[a] The accuracy of the measurements is ± 5%

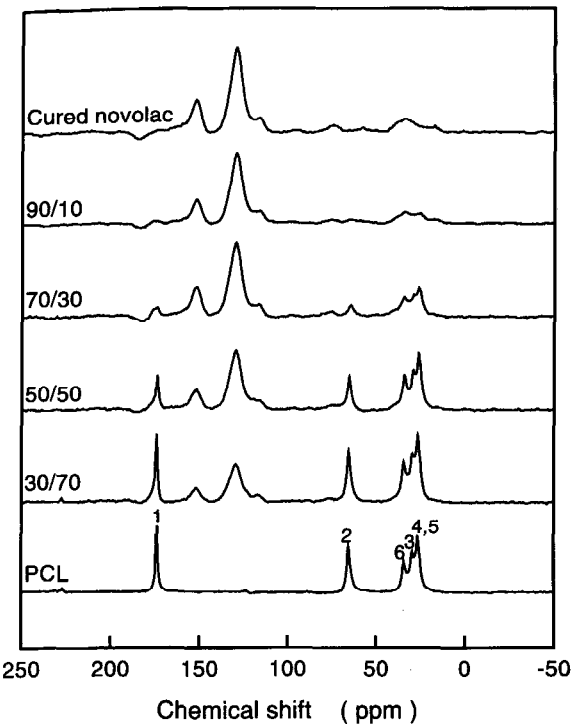


Fig. 5. $^{13}C$ CP/MAS/DD spectra of the 15 wt% HMTA-cured novolac/PCL blends.

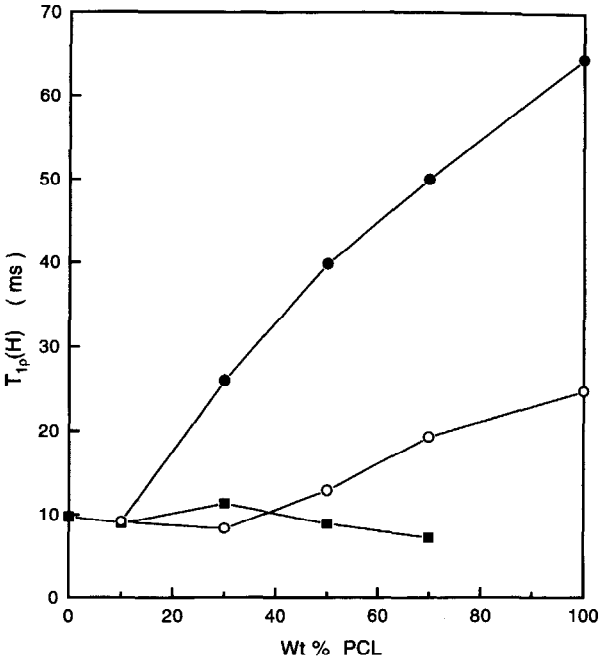


Fig. 6. Composition dependence of $T_{1\rho}(H)$ for the HMTA-cured novolac/PCL blends. Novolac component at 129 ppm (■), amorphous PCL component at 26 ppm (●), and crystalline PCL component at 26 ppm (○).

function model:

$$M_\tau = M_0 \exp(-\tau/T_{1\rho}(H)) \quad (4)$$

Rearranging Eq. (4) and then taking the natural logarithm, we have:

$$\ln(M_\tau/M_0) = -\tau/T_{1\rho}(H) \quad (5)$$

Fig. 4 shows the plots of $\ln(M_\tau/M_0)$ versus spin-locking time, $\tau$, for the selected carbon (at 26 ppm) of PCL and novolac/PCL blends. It can be found that, except for the 70/30 novolac/PCL blend, the experimental data cannot be fitted by a straight line. In fact, the bi-exponential function should be used to simulate the relaxation process for these compositions. The thus obtained $T_{1\rho}(H)$ values are listed in Table 2. From Table 2, two $T_{1\rho}(H)$ components are observed for pure PCL and only one $T_{1\rho}(H)$ is found for pure novolac. This is because that PCL is a semicrystalline polymer while novolac is an amorphous polymer. For a semicrystalline polymer, the proton spin-lattice relaxation rate in the crystalline phase will be different from that in the amorphous phase if the domain sizes of the crystalline/amorphous phases are larger than the spin-diffusion path length within relaxation time. In the PCL case, the shorter component corresponds to the crystalline phase and the longer one (*ca.* 64 ms) to the amorphous phase [24]. Therefore, from the results presented in Tables 1 and 2, the domain sizes of PCL crystalline/amorphous phases are less than the $T_1(H)$ measurement scale of 20–30 nm, while larger than the $T_{1\rho}(H)$ measurement scale of 2–3 nm. It is interesting to find that the carbonyl carbon of PCL has a longer relaxation time than other carbons of PCL, and this phenomenon is more significant in the crystalline region of PCL. In our opinion, this discrepancy is a result of the experimental conditions and does signify actual different relaxation times of different PCL carbons because: (1) there is no hydrogen directly bonding with the carbonyl carbon and therefore the cross-polarization transition of energy is not very efficient for the carbonyl carbon; (2) at low spin-lock time, the experimental error increases (the $T_{1\rho}(H)$ in the crystalline region is determined with data at low spin-lock time).

For the 30/70 and 50/50 novolac/PCL blends, two $T_{1\rho}(H)$ components were also observed for PCL carbons, indicating that these two blends are crystalline. It is interesting to find, in these two blends, that the novolac carbons exhibit another $T_{1\rho}(H)$ which is different from neither that of PCL in the crystalline phase nor that of PCL in the amorphous phase. This result strongly suggests that novolac and PCL are immiscible on the scale of the spin-diffusion path length within $T_{1\rho}(H)$ time for these blends. However, for the 70/30 novolac/PCL blends, only one $T_{1\rho}(H)$ was detected, not only for novolac carbons but also for PCL carbons. Additionally, the $T_{1\rho}(H)$ values of all carbon resonances are the same within the experimental error. Thus, this blend is still miscible on the scale over which spin-diffusion can take place in the time of $T_{1\rho}(H)$.

### 3.2. HMTA-cured novolac/PCL blends

Shown in Fig. 5 are the $^{13}C$ CP/MAS/DD spectra of 15% HMTA-cured novolac, PCL and their blends. Significant

Table 3
$T_1(H)$ values for HMTA-cured novolac, PCL, and their blends[a] (unit: s)

| | PCL | Novolac | | | PCL | PCL/novolac | PCL | |
|---|---|---|---|---|---|---|---|---|
| PCL/novolac | 174 ppm | 152 ppm | 129 ppm | 116 ppm | 66 ppm | 34 ppm | 29 ppm | 26 ppm |
| 100/0 | 1.50 | | | | 1.45 | 1.43 | 1.42 | 1.46 |
| 70/30 | 0.72 | — | 0.72 | — | 0.71 | 0.69 | 0.71 | 0.73 |
| 50/50 | 0.53 | 0.53 | 0.51 | 0.52 | 0.50 | 0.52 | 0.52 | 0.51 |
| 30/70 | — | 0.40 | 0.36 | 0.38 | 0.39 | 0.38 | 0.42 | 0.42 |
| 10/90 | | 0.32 | 0.35 | 0.32 | — | 0.33 | — | 0.32 |
| 0/100 | | 0.25 | 0.27 | 0.25 | | 0.27 | | |

[a] The accuracy of the measurements is ± 5%

changes were noticed in the $^{13}C$ spectra. Firstly, the relative intensity of the un-substituted ortho-carbon in the phenolic rings decreased after curing because partial curing reactions occur at this ortho-position of the phenolic rings [25–27]. Secondly, a slight upfield shift (about 1 ppm) was observed for the C–OH carbon of the cured novolac, indicating that there still exists considerable hydrogen bonding interaction between the C=O groups of PCL and C–OH groups of cured novolac. However, no significant shift was found for the C=O carbon resonance of the PCL component, and this is probably because the shift is too small to be detected under the experimental conditions. At the same time, this also indicates that the relative amount of intermolecular hydrogen bonds has greatly decreased. Finally, the reaction of novolac with crosslinker (HMTA) produces methylene linker between two phenyl ring of novolac. Therefore, no carbon with a different magnetic environment appeared after curing of novolac, and hence no additional resonance line was found in the spectra of cured novolac.

The curing effect on the novolac/PCL blends was further studied by measuring the proton spin-lattice relaxation times. As for the uncured novolac/PCL blends, the $T_1(H)$ magnetization of all resonances decays with delay time by a single-exponential function, thus only one $T_1(H)$ can be obtained for all resonances. The $T_1(H)$ values of the HMTA-cured novolac/PCL blends were calculated through Eq. (2), and the results are listed in Table 3. It is clear that the $T_1(H)$ values of both components are effectively the same for each blend and the value increases monotonically from ca. 0.26 s for the pure cured novolac to ca. 1.45 s for the pure PCL. This indicates homogeneous mixing on the time-scale over which diffusion can take place in $T_1(H)$, i.e. 20–30 nm (from Eq. (3)).

The results of the $T_{1\rho}(H)$ experiment for the HMTA-cured novolac/PCL blends are summarized in Table 4 and Fig. 6. As shown in Fig. 6, the PCL has two $T_{1\rho}(H)$ values; one is for carbons in the crystalline phase and the other for those in the amorphous phase. After blending with cured novolac, three $T_{1\rho}(H)$ were obtained for the 30/70, 50/50 and 70/30 compositions. The third $T_{1\rho}(H)$ is for the carbons of the cured novolac component. When the content of PCL decreases to 10 wt%, all the carbons in the blends relax at an identical rate. Therefore, homogeneous mixing on the scale where the spin-diffusion occurs within the time $T_{1\rho}(H)$ can only take place in the 90/10 cured novolac/PCL blend, and not in the other blends. In addition, from Table 4 and Fig. 6, it can be seen that PCL is still crystalline until the content of PCL in the blend reduces to 30 wt% whereas it is not crystalline in the 90/10 cured novolac/PCL blend. These results are consistent with our previous DSC study [19].

From this n.m.r. study and the previous d.s.c. study on the blends of novolac and PCL, the scales of domain sizes of amorphous phase for the novolac/PCL blends before and after curing with 15 wt% HMTA are summarized in Table 5. It can be seen clearly that the curing causes an increase of the domain sizes in the amorphous phase, and a reduction of miscibility between the two components. The crosslinking reaction between novolac and HMTA resulted in the formation of crosslinked novolac network, which is more stable in the isolated state than in the form of a homogeneous blend.

Table 4
$T_{1\rho}(H)$ values for HMTA-cured novolac, PCL, and their blends[a] (unit: ms)

| | PCL | Novolac | | | PCL | PCL/novolac | PCL | |
|---|---|---|---|---|---|---|---|---|
| PCL/novolac | 174 ppm | 152 ppm | 129 ppm | 116 ppm | 66 ppm | 34 ppm | 29 ppm | 26 ppm |
| 100/0 | 40.5/65.6 | | | | 34.5/63.3 | 28.8/62.1 | 26.8/62.6 | 24.6/64.5 |
| 70/30 | 24.9/46.3 | 5.08 | 7.19 | — | 25.0/53.2 | 19.5/44.4 | 19.5/49.8 | 19.2/50.0 |
| 50/50 | 17.9/39.5 | 7.64 | 8.88 | — | 17.2/44.4 | 12.7/35.1 | 12.7/38.0 | 12.8/39.8 |
| 30/70 | 11.4/24.8 | 12.5 | 11.3 | 12.6 | 8.12/24.0 | 8.42/17.0 | — | 8.30/26.0 |
| 10/90 | — | 9.15 | 8.97 | 9.11 | — | 8.88 | — | 9.15 |
| 0/100 | | 10.2 | 9.76 | 10.5 | | 9.98 | | |

[a] The accuracy of the measurements is ± 5%

Table 5
Domain sizes in amorphous phase for the novolac/PCL blends before and after curing with 15 wt% HMTA

| PCL/novolac | | Domain size (nm) | | |
|---|---|---|---|---|
| | | $T_1(H)$ | DSC | $T_{1\rho}(H)$ |
| 70/30 | uncured | < 20–30 | ≤ 10–15 | > 2–3 |
| | cured | < 20–30 | > 10–15 | > 2–3 |
| 50/50 | uncured | < 20–30 | ≤ 10–15 | > 2–3 |
| | cured | < 20–30 | > 10–15 | > 2–3 |
| 30/70 | uncured | < 20–30 | ≤ 10–15 | < 2–3 |
| | cured | < 20–30 | > 10–15 | > 2–3 |
| 10/90 | uncured | — | ≤ 10–15 | — |
| | cured | < 20–30 | ≤ 10–15 | < 2–3 |

## 4. Conclusions

The intermolecular hydrogen-bonding interaction between the carbonyl groups of PCL and the hydroxyl groups of novolac results in the downfield shift of carbonyl carbon resonance of PCL and the upfield shift of hydroxyl-substituted carbon resonance of novolac. The interaction also broadens the line width of carbonyl carbon resonance. After curing with 15 wt% HMTA, hydrogen-bonding interaction still exists in the blends, whereas the relative amount decreases significantly. Both the uncured and the cured novolac/PCL blends exhibit composition-dependent miscibility. The curing causes an increase of the domain sizes in the amorphous phase, and a reduction of miscibility between the two components. For the uncured blends, novolac and PCL are miscible on the scale of 10–15 nm for 30/70 and 50/50 novolac/PCL compositions, and on the scale of 2–3 nm for 70/30 novolac/PCL composition. As to the cured blends, the intimate mixing occurs on the scale of 20–30 nm for blends for which PCL content is not less than 30 wt%, and occurs on the scale of 2–3 nm for only the 90/10 novolac/PCL composition.

## Acknowledgements

This work was supported by RGC the Earmarked Grand for Research (No. 584/95P), HKUST 96/97. The authors would like to thank Miss Chan Kit Ching for her help in NMR measurements.

## References

[1] Olabisi O, Robeson LM, Shaw MT. Polymer–polymer miscibility New York: Academic Press, 1979.
[2] Shaw TM. In: Walsh DJ, Higgins JS, Maconnachie A, editors. Polymer blends and mixtures, NATO, Advanced Study Institute Series E89 Boston, MA: Martinus Nijhoff Publishers, 1985.
[3] Walsh DJ, Rostami S. Adv Polym Sci 1985;70:119.
[4] Utracki LA. Polymer alloy and blends Munich: Hanser Publishers, 1989.
[5] Mathias LJ, editors. Solid state NMR of polymer New York: Plenum Press, 1991.
[6] McBriety VJ, Packer KJ. Nuclear magnetic resonance in solid polymer Cambridge, UK: Cambridge University Press, 1993.
[7] McBrierty VJ, Douglass DC, Kwei TW. Macromolecules 1978;11:1265.
[8] Grobelny J, Rice DM, Karasez FE, Macknight WJ. (a) Polymer Communication 1990;31:86; (b) Macromolecules 1990;23:2139.
[9] Qin C, Pries ATN, Belfiore LA. Polymer Communication 1990;31:177.
[10] Zhang X, Takegoshi K, Hikichi K. Macromolecules 1992;25:2336.
[11] Zhang X, Takegoshi K, Hikichi K. Polymer 1992;33:712.
[12] Zhang X, Solomon DH. Macromolecules 1994;27:4919.
[13] Feng H, Feng Z, Shen L. Polymer 1993;34:2516.
[14] Papavoine CHM, Maas WEJR, Veeman WS, Buning GHW, Vankan JMJ. Macromolecules 1993;26:6611.
[15] Isasi JR, Cesteros LC, Katime I. Macromolecules 1994;27:2200.
[16] Levon K, Chu E, Ho K-S, Kwei TK, Mao J, Zheng W-Y, Laakso J. Journal of Polymer Science, Polymer Physics 1995;33:537.
[17] Schantz S. Macromolecules 1997;30:1419.
[18] Miyoshi T, Takegoshi K, Hikichi K. Polymer 1997;38:2315.
[19] Zhong Z, Guo Q. Polymer 1997;38:279.
[20] VanderHart DL, Earl WL, Garroway AN. J Magn Reson 1981;44:361.
[21] McBrierty VJ, Douglass DC. Journal of Polymer Science, Macromolecule Review 1981;16:295.
[22] Demco DE, Johansson A, Tegenfeldt J. Solid State Nucl Magn Reson 1995;4:13.
[23] Clauss J, Schmidt-Rohr K, WH. Spiess, Acta Polymer 1993;44:1.
[24] Albert B, Jerome R, Teyssie Ph, Smyth G, McBriety VJ. Macromolecules 1984;17:2552.
[25] Bryson RL, Hatfield GR, Early TA, Palmer AR, Maciel GE. Macromolecules 1983;16:1669.
[26] Hatfield GR, Maciel GE. Macromolecules 1987;20:608.
[27] Chuang I-S, Maciel GE. Macromolecules 1991;24:1025.